Biological Trace Element Research (2024) 202:481–492
https://doi.org/10.1007/s12011-023-03683-3

RESEARCH

Zinc Oxide Nanoparticles Induce Renal Injury by Initiating Oxidative Stress, Mitochondrial Damage and Apoptosis in Renal Tubular Epithelial Cells

Shuang Liu[1] · Han Zhou[1] · Yang Shi[1] · Simeng Yi[1] · Xinyu Wang[1] · Jingyan Li[2] · Bin Liao[2] · Jimin Cao[3] · Guang Li[1]

Received: 7 March 2023 / Accepted: 22 April 2023 / Published online: 29 April 2023

Abstract

Zinc oxide nanoparticles (ZnO NPs) are widely used in many fields due to their unique physicochemical properties. However, the renal toxicity of ZnO NPs and the underlying mechanisms have not been well studied. We found that ZnO NPs induced injury in human renal proximal tubular epithelial cells (HK-2) in a dose- and size-dependent manner, as revealed by CCK-8, LDH and Annexin V-FITC assays. Mechanistically, ZnO NPs promoted oxidative stress and mitochondrial damage by generating ROS and induced apoptosis in HK-2 cells, as evidenced by the upregulation of Bax and Caspase 3 and downregulation of Beclin 1. In vivo, ZnO NPs induced tubular epithelial cell apoptosis and increased serum creatinine, serum urea nitrogen, and urinary protein in mice, suggesting damage to renal structure and function. These findings clarified our understanding of the biological mechanisms underlying ZnO NP-induced renal tubular epithelial cell injury and contributed to estimating the risk of ZnO NPs to the kidney.

Keywords ZnO nanoparticle · HK-2 · Oxidative stress · Mitochondria · Apoptosis · Kidney

Introduction

Nanomaterials are newly developed materials that are widely used in many fields [1]. Zinc oxide nanoparticles (ZnO NPs) are one of the most commonly produced and used nanomaterials due to their unique physiochemical properties [2]. ZnO NPs can protect against ultraviolet radiation and are currently added to many types of sunscreens [3, 4]. ZnO NPs are resistant to high temperatures and inexpensive and have antibacterial properties; thus, they have been widely used in food packaging and even used as food additives [5]. As a new drug carrier, ZnO NPs can be directly injected into the body for cancer treatment [6]. During accidents, industrial workers may even inhale large quantities of ZnO NPs [7]. Thus, ZnO NPs may enter the human body through acute or chronic dermal contact, ingestion and inhalation. In addition, ZnO NPs can accumulate in the body, which increases their safety concerns [8-10].

ZnO NPs have been reported to be toxic, and the kidney is one of the major target organs [11]. Gastrointestinal administration of a single high dose of nano- but not microscale ZnO resulted in proteinaceous casts in the kidneys of mice [12]. Daily gastrointestinal administration of a high dose of ZnO NPs (1,000 mg/kg body weight, for 14

Shuang Liu, Han Zhou and Yang Shi are contributed equally to this work.

✉ Jimin Cao
caojimin@sxmu.edu.cn

✉ Guang Li
liguang@swmu.edu.cn

[1] Department of Cardiology, the Affiliated Hospital of Southwest Medical University and Key Laboratory of Medical Electrophysiology, Ministry of Education & Medical Electrophysiological Key Laboratory of Sichuan Province, and Collaborative Innovation Center for Prevention of Cardiovascular Diseases, Institute of Cardiovascular Research, Southwest Medical University, Luzhou 646000, China

[2] Department of Cardiovascular Surgery, Affiliated Hospital of Southwest Medical University, Southwest Medical University, Luzhou 646000, China

[3] Key Laboratory of Cellular Physiology at Shanxi Medical University, Ministry of Education, and the Department of Physiology, Shanxi Medical University, Taiyuan 030607, China

continuous days) can lead to tubular epithelial cell necrosis and increases in blood urea nitrogen and serum creatinine in rats [13]. This evidence indicates that acute and high doses of ZnO NPs can cause nephrotoxicity. However, it is unclear whether chronic and low-dose oral intake of ZnO NPs, which reflects the real effects of exposure by ingestion, can cause nephrotoxicity. In addition, the kidney is made up of different cell types that have different sensitivities to toxic substances [14]. Therefore, it is critical to select appropriate cell types to elucidate the mechanisms of ZnO NP-induced nephrotoxicity in vitro. Several previous studies have proven the toxic effect of ZnO NPs on HEK293 cells [15-17]. However, a recent study indicated that HEK293 cells are developed from embryonic adrenal precursor cells and are not involved in the main function of the kidney. [18]. In contrast, the HK-2 cell line is derived from human renal proximal tubular epithelial cells, which play a critical role in substance accumulation and tubular reabsorption in the kidney [19]. ZnO NP exposure is toxic to HK-2 cells, but the underlying mechanism has not been fully elucidated [19]. Considering the size-dependent renal effects of nanoparticles, it is still unclear whether smaller ZnO NPs are more toxic to the kidney [20, 21].

To address these questions, ZnO NPs with diameters of 40 nm (ZnO-40) or 100 nm (ZnO-100) were administered daily (34 mg/kg body weight) via oral gavage to adult mice for two months to investigate structural and functional changes in the kidney. In vitro, the effect of ZnO-40 or ZnO-100 exposure on HK-2 cells was examined by cell activity, apoptosis, mitochondrial ROS and membrane potential assays to examine the underlying mechanisms. This study provides a new understanding of the impact of ZnO NPs on the kidney and provides a reference for the use of ZnO NPs in industry and medical practice.

Materials and Methods

Materials

Zinc oxide nanoparticles (ZnO NPs) with diameters of 40 nm (ZnO-40) and 100 nm (ZnO-100) were purchased from Daxinong Nanotechnology Co., Ltd (Changzhou, China). CCK8 detection kit was acquired from HANBIO Company (Shanghai, China). LDH detection kit, penicillin–streptomycin and trypsin were purchased from Beyotime Institute of Biotechnology (Jiangsu, China). MitoSOX and JC-1 were purchased from Invitrogen Company (Carlsbad, CA, USA). AnnexinV-FITC apoptosis/necrosis kit was purchased from BD Biosciences-USA (Franklin Lakes, NJ, USA). HK-2 cells were purchased from Procell Company (Wuhan, China).

Cell Culture

HK-2 cells were cultured in F12 medium supplemented with 10% fetal bovine serum (FBS) and 1% penicillin–streptomycin (P/S) at 37 ℃ and 5% CO_2. Before experiments, the cells were pre-cultured until cell confluence reaching 70–80%.

Preparation and Characterization of ZnO NPs

The ZnO NPs of both sizes were first dispersed in F12 medium and pure water, ultrasonicated and vortexed, then a proper amount of ZnO NPs solution was taken to make a final ZnO NPs concentration of 1 mg/mL. The ZnO NPs solution was ultrasonicated and vortexed again to make the particle dispersed evenly. The hydrodynamic diameters and Zeta potentials of ZnO NPs diluted in pure water and F12 medium were measured by dynamic light scattering (DLS) and Zetasizer Nano System (Malvern instruments, UK).

Cell Viability Assay

The effects of ZnO NPs on the viability of HK-2 cells was evaluated by CCK-8 assay. HK-2 cells were seeded into 96 well plates at a density of 1×10^4 cells/well and then exposed to 0, 5, 10, 15 and 20 μg/mL ZnO NPs. After 24-h or 48-h exposure, 10% CCK8 detection reagent was added into wells and cell viability was detected at 450 nm using Cell Imaging Multimode Reader.

Measurement of Lactate Dehydrogenase Leakage

HK-2 cells were seeded into a 96-well plate at a density of 1×10^4 cells/well, then exposed to 0, 5, 10, 15 and 20 μg/mL ZnO NPs. After 24-h exposure, cells were centrifuged at 400 g for 5 min. The supernatant (120 μL) of each sample was incubated with 60 μL lactate dehydrogenase (LDH) working solution in the dark for 30 min, and the absorbance at 490 nm was detected using Cell Imaging Multimode Reader.

AnnexinV-FITC/PI Apoptosis Assay

HK-2 cells were seeded on a 6-well plate and cultured until confluence to 80%, then cells were treated with F12 complete medium containing ZnO-40 or ZnO-100 at different concentrations (0, 10 and 15 μg/mL) for 24 h. Cells were then digested with 0.25% trypsin, filtered, fixed with 1×binding buffer, and stained with 5 μL Annexin V-FITC/PI at room temperature for 15 min without light. The

apoptotic cells were detected by flow cytometry. Blank and Annexin V-FITC/PI alone tubes were used as controls.

Western Blotting

HK-2 cells were seeded into 6-well plates at a density of 2×10^5 cells/well and exposed to ZnO NPs at concentrations of 0, 10 and 15 μg/mL for 24 h. Cells were rinsed twice with ice-cold PBS and treated with 1% protease inhibitor and phosphatase inhibitor. Cells were then scraped and lysed on ice for 30 min and ultrasonic for 2 min. Cell lysates were centrifuged at 12,000 rpm for 15 min at 4 ℃, and the supernatants were collected. Cell proteins were separated by SDS-PAGE and transferred onto polyvinylidene difuoride membranes and blocked with 5% nonfat milk for 2 h. The membrane was incubated overnight at 4 ℃ with primary antibodies respectively against Caspase 3 (dilution 1:2000), Bax (dilution 1:2000), Bcl-2 (dilution 1:2000), Beclin 1 (1:1000) and β-actin (1:2000). The membranes were then washed with Tris-buffered saline containing Tween 20 (TBST) and incubated at room temperature with horseradish peroxidase (HRP)-conjugated secondary antibodies for 1 h. Proteins were detected using an enhanced chemiluminescence (ECL) kit and an automatic chemiluminescence image analysis system. Quantitative analysis was performed using ImageJ software.

Detection of Mitochondrial ROS in HK-2 Cells

HK-2 cells were seeded in a confocal glass dish and exposed to ZnO-40 or ZnO-100 at 0, 10 and 15 μg/mL for 3 h. MitoSox was diluted with HBSS at 1:1000 and incubated for 10 min, with hoechst33342 for 2 min, cells were then washed with PBS and photographed under a fluorescence microscope.

Measurement of Mitochondrial Membrane Potential

HK-2 cells were seeded on confocal glass dishes to grow and exposed ZnO-40 or ZnO-100 at 0, 10, and 15 μg/mL for 3 h. JC-1 stock solution was diluted with serum-free F12 medium to a final concentration of 5 μg/mL. Cells were incubated with working JC-1 solution at 37 ℃ for 10 min and then with hoechst 33,342 at 37 ℃ for 2 min. After staining, cell pictures were taken with a confocal microscope, JC-1 monomers and JC-1 aggregates were visualized respectively with excitation light of 488 nm and 568 nm. The ratio of red fluorescence intensity to green fluorescence intensity was used to represent the level of mitochondrial membrane potential.

In vivo Experiments

Eight-week-old C57BL/6 male mice were purchased from Chengdu Yaokang Company (Chengdu, China). Mice were fed in a clean animal laboratory at 20–24 ℃, humidity 40–70%, 12:12 h light/dark cycle, and had free access to water and regular SPF-grade adult mice breeding feed (HUANYU BIO, BeiJing). After one week of adaptation, mice were administrated with ZnO-40 at 34 mg/kg by oral gavage daily for 2 months. The mice administrated with same amount of water were used as control. The mice were randomized into ZnO-40 group and control group (n = 6 in each group). Urines were collected with 1.5-mL EP tubes before the end of the experiment. Mice were anesthetized with 1% pentobarbital, blood samples were collected from the eyeballs, and kidneys were harvested and fixed with 10% neutral formaldehyde for further experiments. The animal use protocol was approved by the Ethics Committee of Southwest Medical University for animal experiments (approval No. 20190306–012).

TUNEL Assay

DNA fragmentation represents the characteristics of late apoptosis, and the TUNEL (TdT-mediated dUTP nick end labeling) apoptosis detection kit can be used to detect the fragmentation of nuclear DNA in tissue cells during apoptosis. TUNEL death detection kit was used to detect apoptotic cells in mice renal paraffin sections according to the manufacturer's instructions, nuclei were stained with DAPI, and the fluorescent stains were captured with a confocal microscope.

Blood and Urine Tests

Mice blood samples were collected from the control and ZnO NPs-treated mice, kept stillness at 4 °C for 30 min to let coagulated and then centrifuged at 3,000 rpm for 15 min to separate the serum. Mice urines were collected and centrifuged at 3,000 rpm for 15 min. Blood urea nitrogen (BUN) and creatinine levels, and urine protein levels were measured using an automatic biochemical detector.

Histology

Mice kidneys were harvested and fixed with 10% neutral formaldehyde, dehydrated with a full-automatic dehydrator, and embedded in paraffin. Four μm sections were cut with a microtome and stained with hematoxylin and eosin (H&E). Structural changes were examined under a microscope.

Statistical Analysis

All data were expressed as mean ± standard deviation (SD). All values were obtained from at least three independent experiments. Statistical significance was evaluated using one-way analysis of variance (ANOVA). $P < 0.05$ was considered statistically significant.

Results

Physiochemical Characterization of ZnO NPs

The hydrodynamic size and zeta potential of ZnO NPs (ZnO-40 and ZnO-100) in different dispersion media were measured. As shown in Fig. 1, the zeta potentials of ZnO-40 and ZnO-100 in pure water were reduced, and their dispersion was improved. ZnO NPs showed slight aggregation in the medium. ZnO-40 and ZnO-100 exhibited homogeneous size distributions.

Cytotoxicity of ZnO NPs in HK-2 Cells

A CCK8 assay was performed to evaluate the cytotoxicity of ZnO NPs in HK-2 cells. The cells were treated with different concentrations of ZnO-40 or ZnO-100 for 24/48 h followed by the CCK8 assay. Compared with that in the control group, ZnO-40 and ZnO-100 induced dose- and time-dependent reductions in cell viability, and the cytotoxicity of ZnO-40 was greater than that of ZnO-100 (Figs. 2 A, S1 A).

An LDH leak assay was performed to evaluate the membranous toxicity of ZnO NPs in HK-2 cells. The results showed that ZnO-40 and ZnO-100 significantly increased LDH leakage in a concentration-dependent manner (Fig. 2 B), indicating that ZnO NPs could damage membrane integrity.

After 24 h of ZnO NP exposure, ZnO-40 had smaller IC50 values than ZnO-100 (18 and 33.2 μg/mL, respectively) (Fig. 2 C), and after 48 h of treatment with ZnO-40 and ZnO-100, the IC50 values decreased to 16.5 and 28.6 μg/mL, respectively (Fig. S1 C).

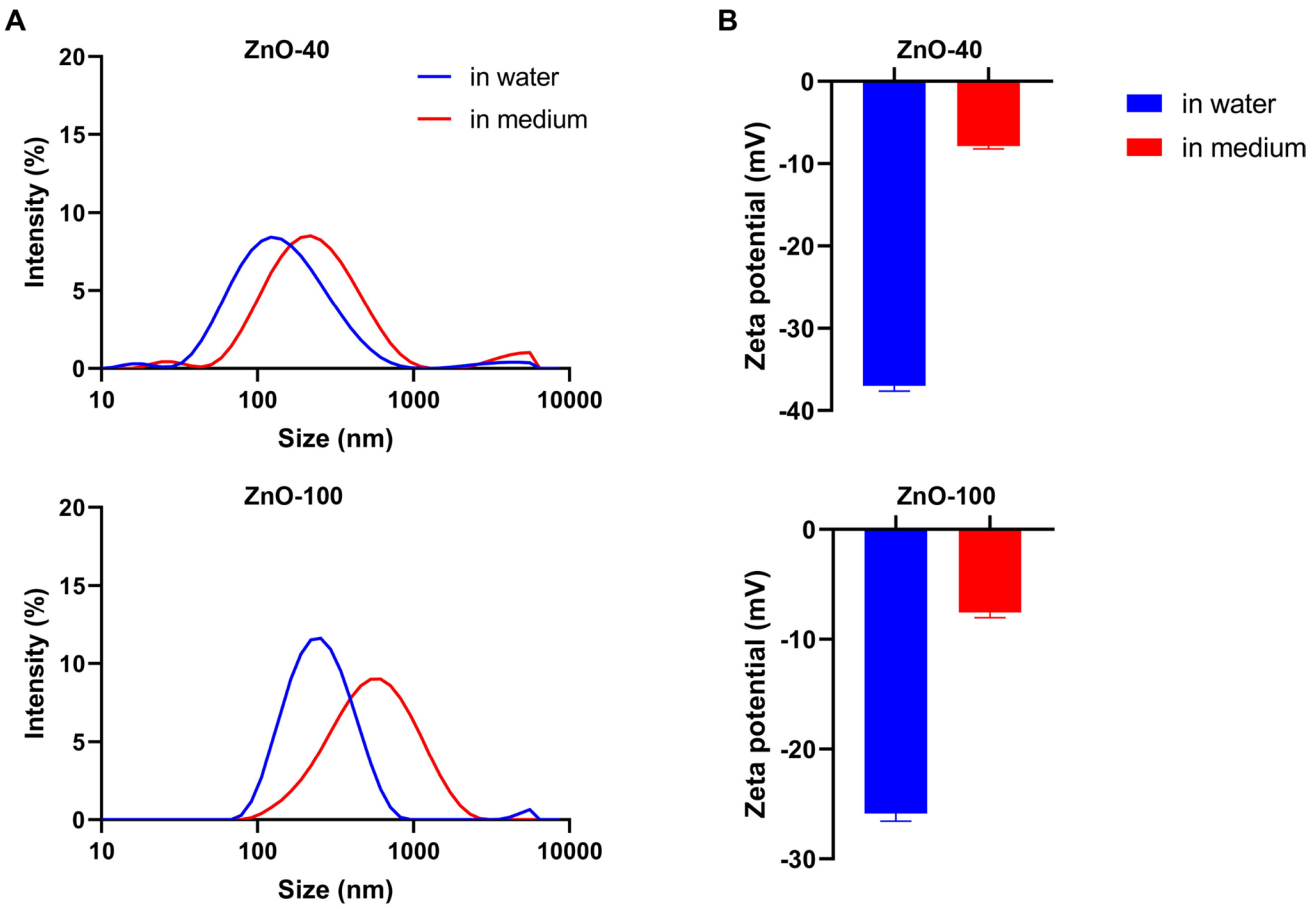

Fig. 1 Characterization of ZnO NPs. (**A**) Hydrodynamic diameters of ZnO-40 and ZnO-100 in water and culture medium. (**B**) Zeta potentials of ZnO-40 and ZnO-100 in water and culture medium

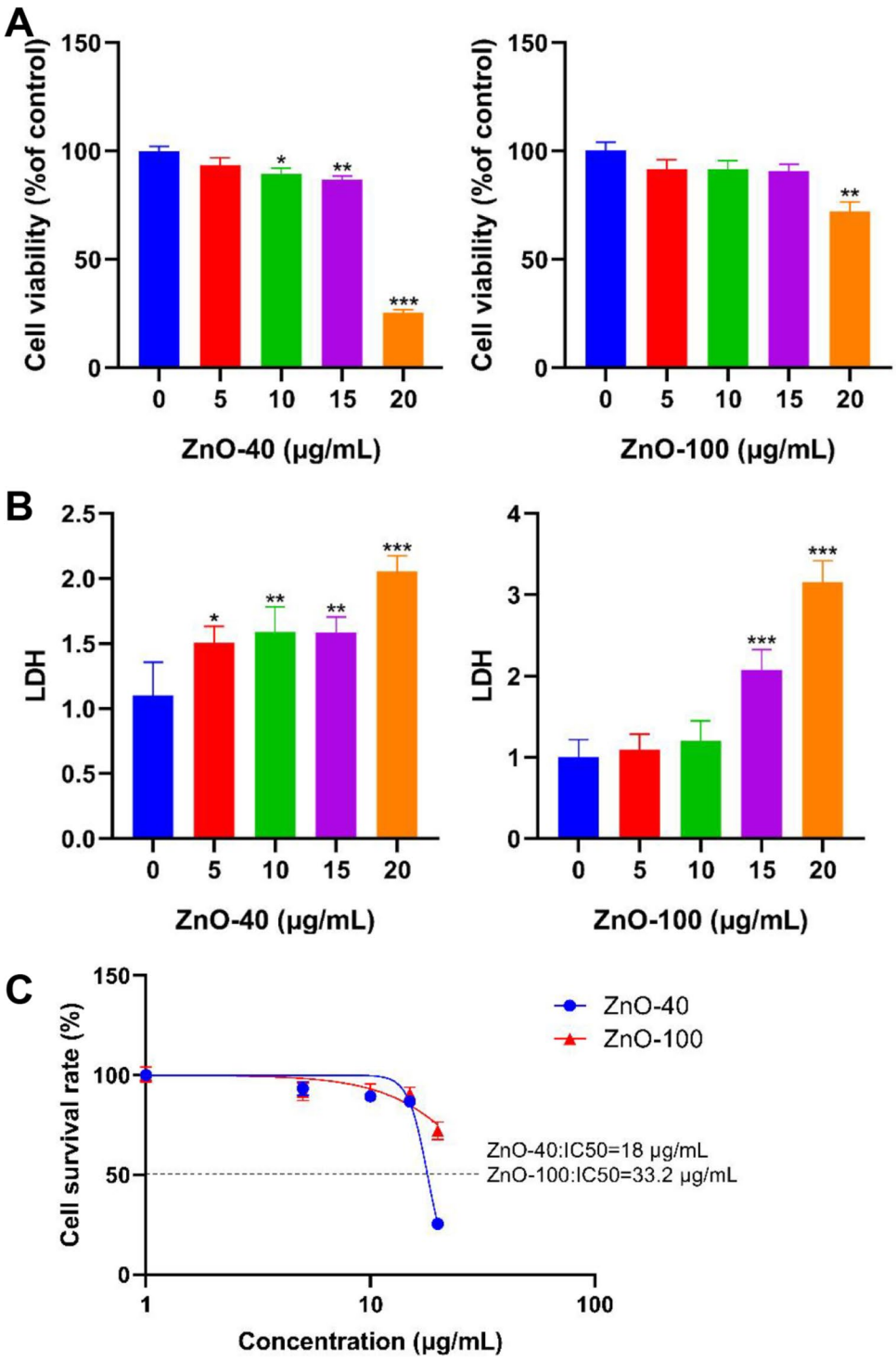

Fig. 2 Cytotoxicity of ZnO NPs in HK-2 cells. (**A**) CCK8 assay showing the effects of ZnO-40 and ZnO-100 (0, 5, 10, 15 and 20 μg/mL) on the viability of HK-2 cells at 24 h. (**B**) The LDH leak assay showing membranous injury induced by ZnO-40 and ZnO-100 (0, 5, 10, 15 and 20 μg/mL) in HK-2 cells. (**C**) IC50 values in HK-2 cells treated with ZnO-40 and ZnO-100 for 24 h

HK-2 Cell Apoptosis Induced by ZnO NPs

Annexin V-FITC/PI apoptosis assays were performed using flow cytometry. During the early stage of apoptosis, phosphatidylserine (PS) in the cell membrane moves from the inner side to the outer side of the lipid membrane. Annexin V has a high affinity for PS and can bind to the cell membrane during the early stage of apoptosis. PI cannot penetrate the cell membrane, but PI can penetrate the cell membrane and stain the nucleus red in cells during the middle and late stages of apoptosis. Thus, Annexin V-FITC/PI-labeled cells can indicate apoptosis and necrosis. Compared with that in control cells, apoptosis in ZnO-40 (10 μg/mL)-treated HK-2 cells was significantly

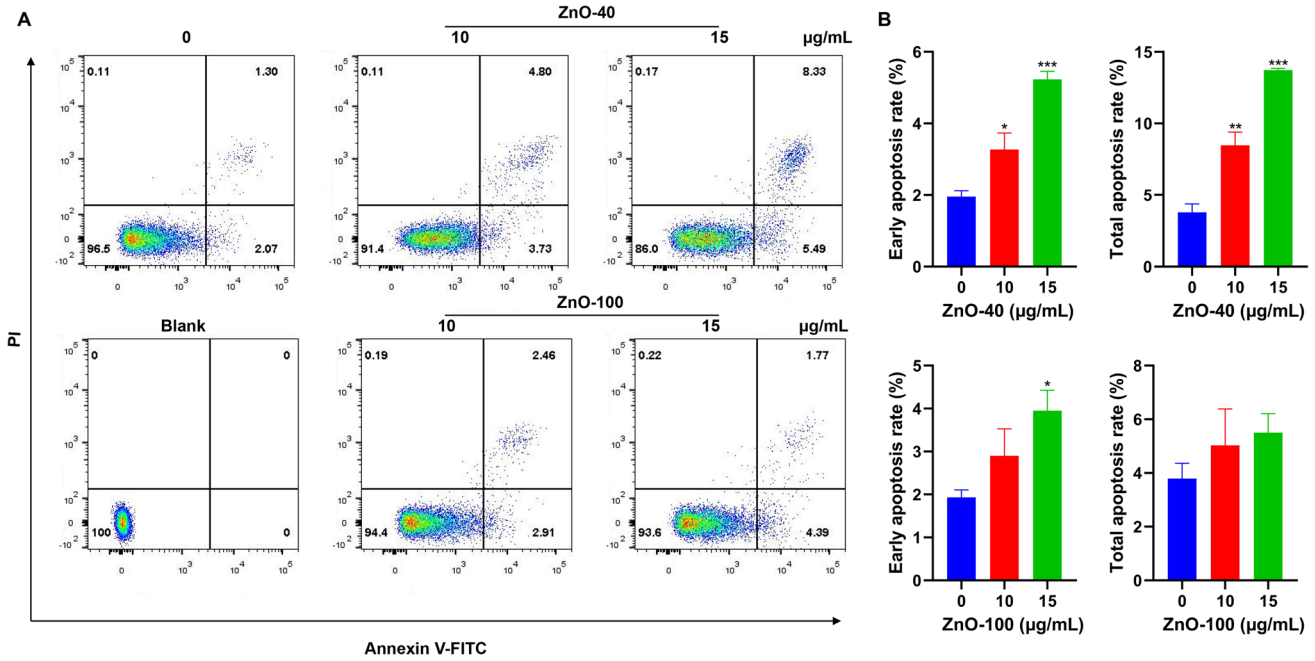

Fig. 3 Flow cytometry to detect apoptosis in HK-2 cells induced by ZnO-40 and ZnO-100 (0, 10, and 15 μg/ml for 24 h). (**A**) Original representative data. (**B**) Statistical results (n = 3)

increased (Fig. 3). However, ZnO-100 (15 μg/mL)-treated HK-2 cells only showed early apoptosis (Fig. 3), suggesting that the effect of ZnO-40 on inducing apoptosis was greater than that of ZnO-100.

Changes in Apoptosis-Related Proteins in HK-2 Cells Induced by ZnO NPs

ZnO-40 treatment (10 and 15 μg/mL) for 24 h significantly changed the protein expression levels of Bax, Bcl-2,

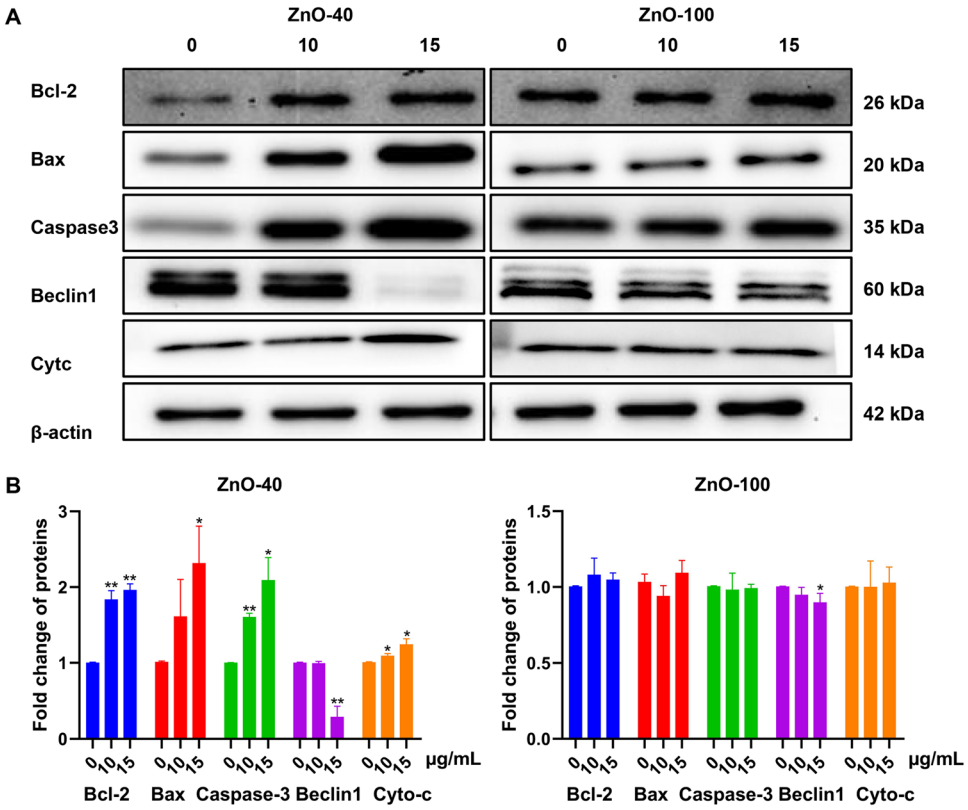

Fig. 4 Western blots showing apoptosis-related proteins (Bax, Bcl-2, Caspase-3, Beclin-1, Cyto-C) in HK-2 cells treated with ZnO-40 and ZnO-100. (**A**) Original representative data. (**B**) Statistical results (n = 3)

Caspase-3, Beclin-1 and Cyto-C in a concentration-dependent manner (Fig. 4), while the changes in these proteins were significantly less in ZnO-100 (10 and 15 μg/mL)-treated cells than in ZnO-40-treated cells (Fig. 4), indicating that ZnO-40 was more powerful than ZnO-100 in inducing HK-2 cell apoptosis.

Induction of Mitochondrial ROS in HK-2 Cells by ZnO NPs

Compared with control cells, ZnO NP (10 and 15 μg/mL)-treated HK-2 cells showed increased ROS generation (Fig. 5). In addition, ZnO-40 induced higher levels of ROS than ZnO-100 in HK-2 cells (Fig. 5), suggesting that ZnO-40 was more powerful than ZnO-100 in inducing mitochondrial ROS.

Mitochondrial Damage in HK-2 Cells Induced by ZnO NPs

In normal cells, mitochondrial membrane potential is high, and JC-1 aggregates in the mitochondrial matrix to form a polymer, which can produce red fluorescence. In the early stage of apoptosis, mitochondrial membrane potential is low, JC-1 cannot aggregate in the mitochondrial matrix, and JC-1 is a monomer that can produce green fluorescence. Compared with that of control cells, the mitochondrial membrane potential of HK-2 cells treated with ZnO-40 and ZnO-100 (10 and 15 μg/mL) was significantly decreased (Fig. 6), and this decrease was more obvious in ZnO-40-treated cells than in ZnO-100-treated cells (Fig. 6), suggesting that ZnO-40 is more toxic than ZnO-100 to mitochondria.

Renal Histological Changes Induced by ZnO NPs in Mice

HE staining of mouse renal tissue sections showed that ZnO-40 damaged the structure of the kidney, especially the renal tubules. Compared with those in control renal tissue, the tubules of ZnO-40-treated mice showed disordered arrangement, cellular degeneration, and reduced numbers of nuclei in tubular epithelial cells (Fig. 7). The damage to the glomerulus induced by ZnO-40 was characterized by disturbances in cellular arrangement and widened renal capsules (Fig. 7). However, compared with that in the control group, the renal structural damage induced by ZnO-100 was not significant (Figure S2).

Apoptosis in Mouse Kidney Tissues Induced by ZnO NPs in vivo

TUNEL staining was performed to visualize apoptosis in the kidney tissues of mice. The results showed that the numbers of apoptotic cells in the kidney tissues of ZnO-40-treated mice were significantly higher than those in control mice (Fig. 8 A, B). However, the number of apoptotic cells in the ZnO-100-treated group did not change significantly

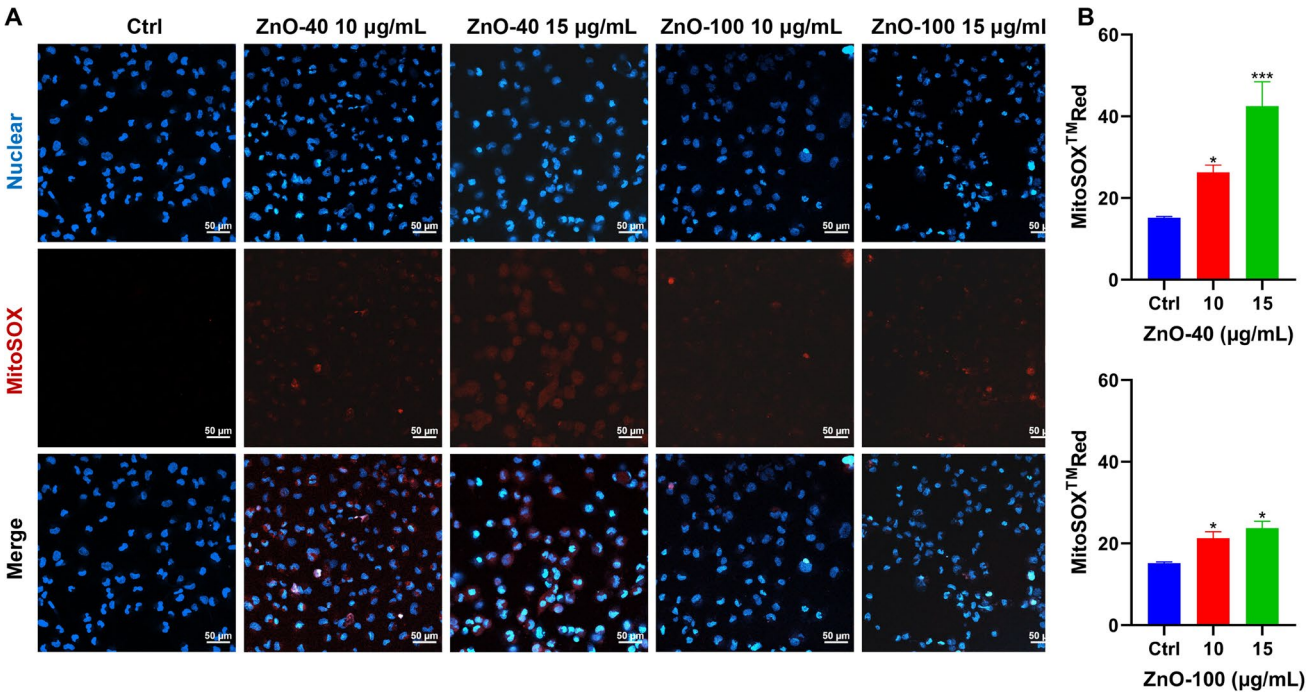

Fig. 5 Measurement of mitochondrial ROS levels in HK-2 cells using MitoSOX Red staining. Before being stained, the cells were exposed to 0, 10 and 15 μg/mL ZnO-40 and ZnO-100 for 3 h. DAPI (blue) was used for nuclear staining

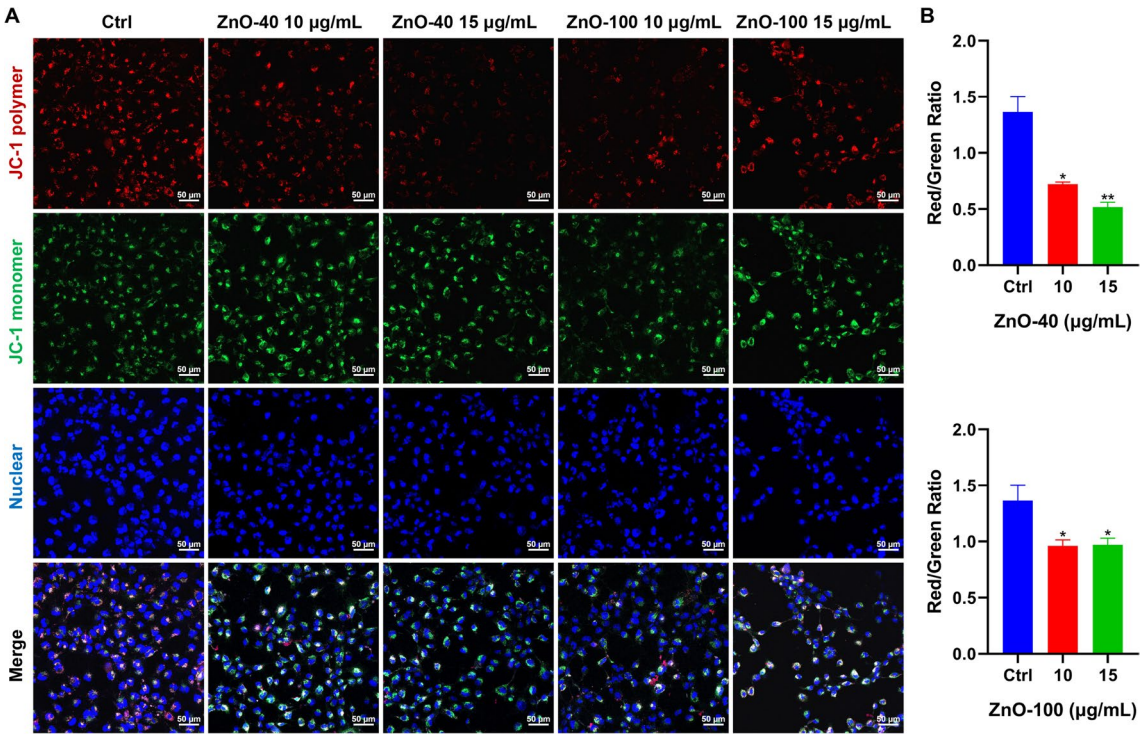

Fig. 6 JC-1 staining showing the disruption of mitochondrial membrane potential induced by ZnO NPs in HK-2 cells. DAPI (blue) was used for nuclear staining

(Figure S3 A, B), indicating that smaller ZnO-NPs more easily induced apoptosis in vivo.

Biochemical Changes in Blood and Urine Induced by ZnO NPs in Mice

Serum creatinine and urea nitrogen levels are common indicators of kidney function in the clinical. The results showed that after oral administration of ZnO-40, the levels of serum creatinine, urea nitrogen and urine protein were significantly elevated compared with those in control mice (Fig. 8 C). However, these parameters did not significantly change in ZnO-100-treated mice (Fig. S3 C), suggesting that ZnO-40 is more toxic to renal function than ZnO-100.

Discussion

Recent studies have indicated that many nanoparticles, including ZnO NPs, preferentially accumulate in the kidney after entering the body [8, 9]. Elimination of ZnO NPs by the kidney is the most effective excretion pathway [22]. Although acute and high-dose (500–1000 mg/kg body weight) exposure to ZnO NPs has been shown to be toxic to the kidney, our study is the first to report nephrotoxic evidence following two months of daily intragastric administration of two different sizes (40 nm and 100 nm) of ZnO NPs (34 mg/kg body weight) in C57 mice. After 2 months of oral exposure to ZnO, we did not find obvious manifestations of kidney damage in response to ZnO-100. However, exposure to ZnO-40 caused overt renal tubular epithelial cell apoptosis and a significant increase in blood creatinine, blood urea nitrogen, and urinary protein, which indicated damage to the reabsorption abilities of proximal tubular epithelial cells. Our observation is consistent with a previous report suggesting that the proximal convoluted tubule was the main target of ZnO NPs [13].

To elucidate the mechanisms of apoptosis caused by ZnO NPs, we used HK-2 cells, the representative cell line of proximal tubular epithelial cells of the human renal cortex, to investigate the size-dependent effects and the underlying pathways. Our CCK-8 and LDH leak assays showed that ZnO-40 and ZnO-100 significantly reduced the viability of HK-2 cells and destroyed the integrity of cell membranes in a concentration- and size-dependent manner. Notably, ZnO-40 showed greater toxicity than ZnO-100, indicating that smaller ZnO NPs are more toxic to the kidney. The flow cytometry results showed that ZnO-40 (15 μg/mL) significantly increased the level of early and late apoptosis in HK-2 cells, whereas the same concentration of ZnO-100 only caused early apoptosis. Since the mitochondria-related

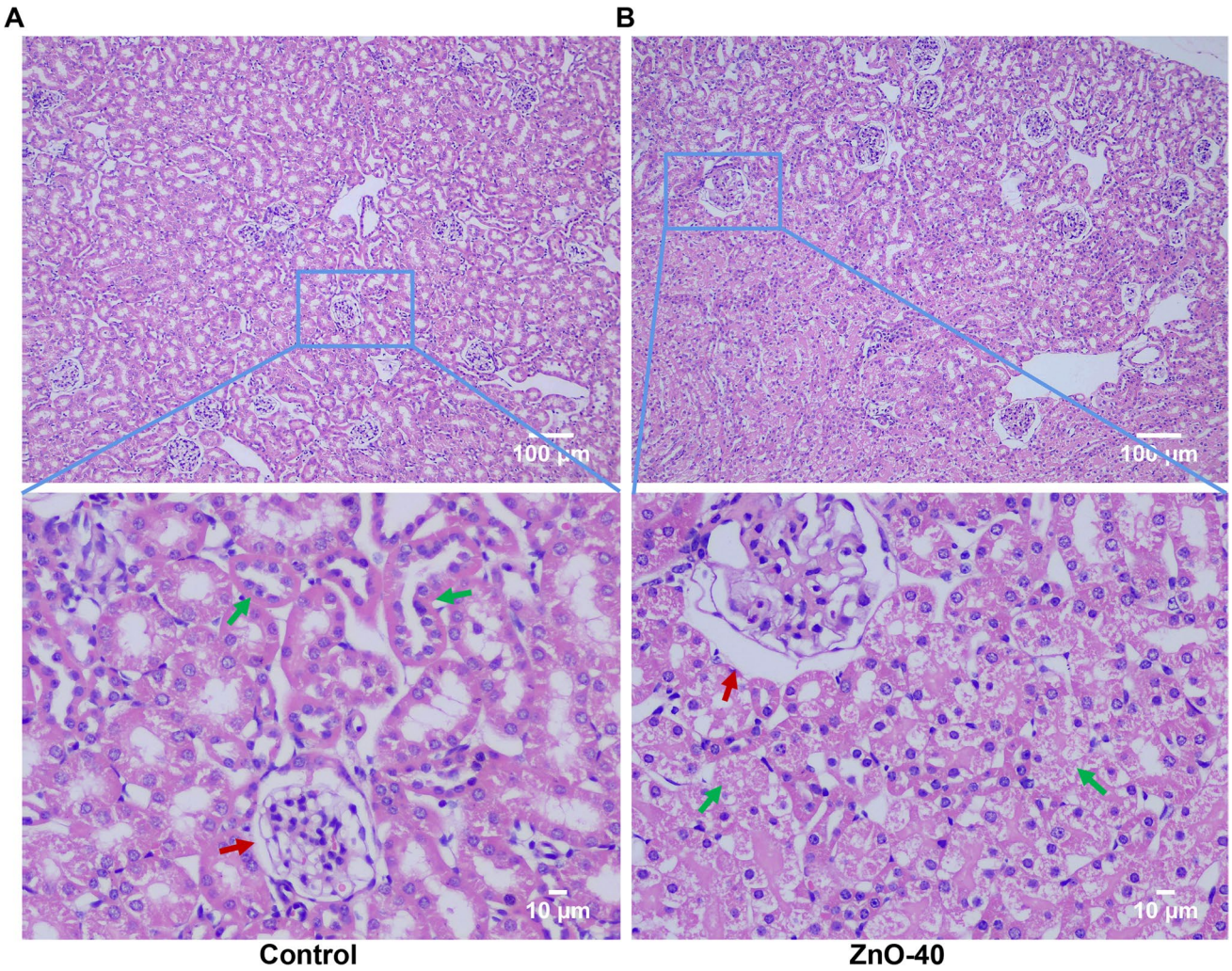

Fig. 7 H&E staining of mouse kidney tissues. (**A**) Control. Normal structures of the glomerulus (red arrow) and renal tubules (green arrows) were observed. (**B**) Oral ingestion of ZnO-40 (34 mg/kg/day for 2 months). Widened renal vesicles (red arrow), disordered arrangement of renal tubules, degeneration of renal tubular epithelial cells and the loss of tubule cell nuclei were observed (green arrows)

signaling pathway is involved in the toxicity caused by ZnO NPs exposure [23], we examined the expression levels of signaling proteins. We observed increased expression of Bax, Bcl-2, Caspase 3 and Cyto-C but decreased expression of Beclin-1 in HK-2 cells after exposure to 15 μg/mL ZnO-40, whereas ZnO-100 exposure only caused a decrease in Beclin-1. The upregulation of Bax, Caspase 3 and Cyto-C expression indicates activation of the mitochondrial-dependent pathway. Bcl-2 not only plays a key role in survival by inhibiting apoptosis but also inhibits autophagy proteins by inhibiting Beclin-1 to regulate the transition between autophagy and apoptosis [24-26]. Bcl-2 inhibits beclin-1-dependent autophagy, which in turn promotes apoptosis [27].

NPs have been shown to be deposited on the cell surface or inside suborganelles and induce a cascade of oxidative stress signaling, ultimately leading to oxidative stress and decreased functions in different cell types [28-30]. Oxidative stress is thought to be the main mechanism of NP-induced cell and tissue toxicity, which can be attributed to the smaller size and larger specific surface area of NPs [31]. Mitochondria are one of the main target organelles of oxidative stress-induced damage [32]. In cardiomyocytes, ZnO NPs can promote mitochondrial ROS generation by depolarizing mitochondrial membranes and destroying electron transport, leading to a decrease in mitochondrial membrane potential, which is a sign of early apoptosis [10]. We found that ZnO-40

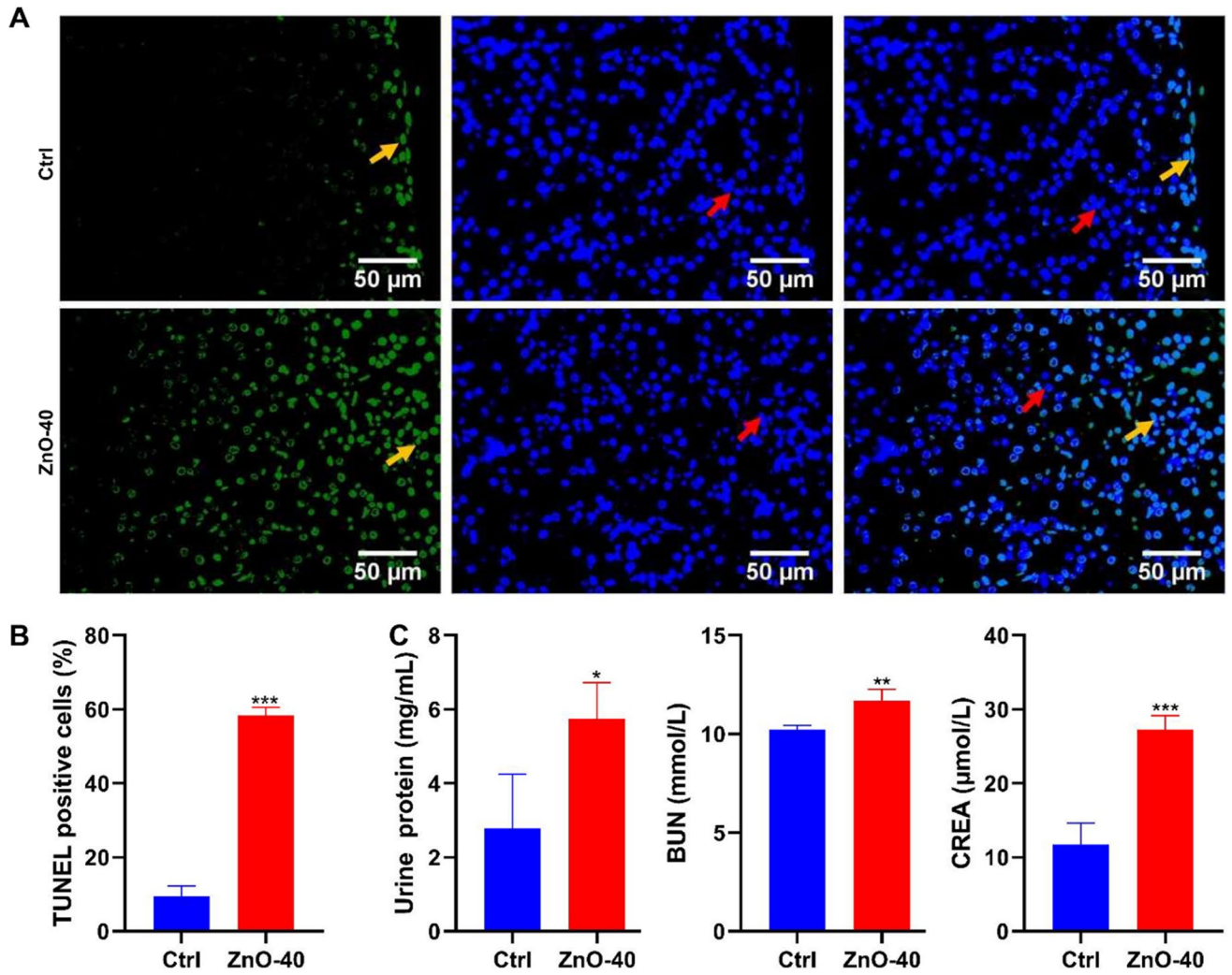

Fig. 8 (**A**, **B**) TUNEL staining of kidney tissues. Green, TUNEL-positive nuclei. Blue, DAPI-positive nuclei. Red arrow, normal cells. Yellow arrow, apoptotic cells. (**C**) Blood and urine results

induced higher levels of ROS in HK-2 cells than ZnO-100, suggesting that ZnO-40 is more powerful at causing oxidative stress. Accordingly, the decrease in the mitochondrial membrane potential in HK-2 cells was more significant in the ZnO-40-treated group than in the ZnO-100 group, which further indicates that the renal toxicity of ZnO NPs depends on particle size.

After ingestion, ZnO NPs can reach the blood circulation from the gastrointestinal tract and accumulate in the kidneys [33]. ZnO NPs with smaller sizes take less energy than larger NPs to be taken up by kidney cells [34]. In addition, cellular uptake of smaller ZnO NPs can be further facilitated by clathrin-mediated endocytosis [35]. As a result, smaller ZnO NPs will more easily accumulate in the kidney. Considering the higher toxicity of ZnO-40 NPs than ZnO-100 NPs, it is reasonable that chronic ingestion of ZnO-40 NPs compromises kidney function more severely in mice than larger particles. Our observation is consistent with previous reports suggesting that smaller ZnO NPs are more toxic [36, 37]

Conclusion

Chronic oral ingestion of ZnO NPs induces significant renal injury in mice in vivo and is toxic to human renal tubular epithelial HK-2 cells in vitro. The renal toxicities of ZnO NPs are mainly characterized by tubular epithelial cell degeneration and apoptosis. The major toxicity mechanisms involve ROS generation, oxidative stress and activation of the mitochondrial apoptotic pathway in tubular epithelial cells. ZnO NPs with smaller particle size (ZnO-40) have greater toxicity than larger particles (ZnO-100), indicating that the renal toxicities of ZnO NPs depend on particle size. This study raises a

warning regarding the application of ZnO NPs in industry and medical practice and suggests that ZnO NPs have renal toxicity, especially in those with renal diseases and reduced renal function.

Supplementary Information The online version contains supplementary material available at https://doi.org/10.1007/s12011-023-03683-3.

Acknowledgements This work was supported by the National Natural Science Foundation of China (81870261, 82170523), Sichuan Youth Science and Technology Innovation Research Team (2020JDTD0024), Sichuan Science and Technology Program (xtcx2016-14, 2022YFS0610), and Shanxi Medical Key Science and Technology Project Plan of China (2020XM01).

Author contributions Shuang Liu: Conceptualization, Methodology, Investigation, Formal Analysis, Writing - Original DraftHan Zhou: Software, Investigation, Writing - Original DraftYang Shi: Visualization, InvestigationSimeng Yi: Software, ValidationXinyu Wang: Software, ValidationJingyan Li: Resources, SupervisionBin Liao: VisualizationJimin Cao: Conceptualization, Funding Acquisition, Resources, Supervision, Writing - Review & EditingGuang Li: Conceptualization, Funding Acquisition, Resources, Supervision, Writing - Review & Editing All authors reviewed the manuscript

Data Availability The data that support the findings of this study are available from the corresponding author upon reasonable request.

Declarations

Competing interests The authors declare no competing interests.

Disclosure The authors report no conflicts of interest in this work.

References

1. Ray PC, Yu H, Fu PP (2009) Toxicity and environmental risks of nanomaterials: challenges and future needs [J]. J Environ Sci Health C Environ Carcinog Ecotoxicol Rev 27(1):1–35
2. Diez-Pascual AM, Diez-Vicente AL (2014) ZnO-reinforced poly(3-hydroxybutyrate-co-3-hydroxyvalerate) bionanocomposites with antimicrobial function for food packaging [J]. ACS Appl Mater Interfaces 6(12):9822–9834
3. Gulson B, Mccall M, Korsch M et al (2010) Small amounts of zinc from zinc oxide particles in sunscreens applied outdoors are absorbed through human skin [J]. Toxicol Sci 118(1):140–149
4. Gulson B, Wong H, Korsch M et al (2012) Comparison of dermal absorption of zinc from different sunscreen formulations and differing UV exposure based on stable isotope tracing [J]. Sci Total Environ 420:313–318
5. Esmailzadeh H, Sangpour P, Shahraz F et al (2016) Effect of nanocomposite packaging containing ZnO on growth of Bacillus subtilis and Enterobacter aerogenes [J]. Mater Sci Eng C Mater Biol Appl 58:1058–1063
6. Ruenraroengsak P, Kiryushko D, Theodorou IG et al (2019) Frizzled-7-targeted delivery of zinc oxide nanoparticles to drug-resistant breast cancer cells [J]. Nanoscale 11(27):12858–12870
7. Monsé CA-O, Hagemeyer O, Raulf M, et al (2018) Concentration-dependent systemic response after inhalation of nano-sized zinc oxide particles in human volunteers. J Part Fibre Toxicol 15(8)
8. Baek M, Chung HE, Yu J et al (2012) Pharmacokinetics, tissue distribution, and excretion of zinc oxide nanoparticles [J]. Int J Nanomed 7:3081–3097
9. Fujiharaa J, Tongub M, Fujitaf Y et al (2014) Distribution and toxicity evaluation of ZnO dispersion nanoparticles in single intravenously exposed mice [J]. J Med Invest 62:45–50
10. Moris D, Spartalis M, Tzatzaki E et al (2017) The role of reactive oxygen species in myocardial redox signaling and regulation [J]. Ann Transl Med 5(16):324
11. Esmaeillou M, Moharamnejad M, Hsankhani R et al (2013) Toxicity of ZnO nanoparticles in healthy adult mice [J]. Environ Toxicol Pharmacol 35(1):67–71
12. Wang B, Feng WY, Wang TC et al (2006) Acute toxicity of nano- and micro-scale zinc powder in healthy adult mice [J]. Toxicol Lett 161(2):115–123
13. Yan G, Huang Y, Bu Q et al (2012) Zinc oxide nanoparticles cause nephrotoxicity and kidney metabolism alterations in rats [J]. J Environ Sci Health A Tox Hazard Subst Environ Eng 47(4):577–88
14. Pujalté I, Passagne I, Brouillaud B, et al (2011) Cytotoxicity and oxidative stress induced by different metallic nanoparticles on human kidney cells [J]. Part Fibre Toxicology 8(10)
15. Guan R, Kang T, Lu F, et al (2012) Cytotoxicity, oxidative stress, and genotoxicity in human hepatocyte and embryonic kidney cells exposed to ZnO nanoparticles. J Nanoscale Res Lett 7 (1):602
16. Lin YF, Chiu IJ, Cheng FY et al (2016) The role of hypoxia-inducible factor-1alpha in zinc oxide nanoparticle-induced nephrotoxicity in vitro and in vivo [J]. Part Fibre Toxicol 13(1):52
17. Yang Y, Song Z, Wu W et al (2020) ZnO Quantum Dots Induced Oxidative Stress and Apoptosis in HeLa and HEK-293T Cell Lines [J]. Front Pharmacol 11:131
18. Lin YC, Boone M, Meuris L et al (2014) Genome dynamics of the human embryonic kidney 293 lineage in response to cell biology manipulations [J]. Nat Commun 5:4767
19. Gunness P, Aleksa K, Kosuge K et al (2010) Comparison of the novel HK-2 human renal proximal tubular cell line with the standard LLC-PK1 cell line in studying drug-induced nephrotoxicity [J]. Can J Physiol Pharmacol 88(4):448–455
20. Abdelhalim MAK, Jarrar BM (2011) Renal tissue alterations were size-dependent with smaller ones induced more effects and related with time exposure of gold nanoparticles. Lipids Health Dis 10:163
21. Kang T, Guan R, Chen X, et al (2013) In vitro toxicity of different-sized ZnO nanoparticles in Caco-2 cells. J Nanoscale Res Lett 8(1):496
22. Burns AA, Vider J, Ow H et al (2009) Fluorescent silica nanoparticles with efficient urinary excretion for nanomedicine [J]. Nano Lett 9(1):442–448
23. Wang L, Chen C, Guo L et al (2018) Zinc oxide nanoparticles induce murine photoreceptor cell death via mitochondria-related signaling pathway [J]. Artif Cells, Nanomed Biotechnol 46(sup1):1102–1113
24. Pattingre S, Tassa A, Qu X et al (2005) Bcl-2 Antiapoptotic Proteins Inhibit Beclin 1-Dependent Autophagy [J]. Cell 122(6):927–939
25. Samuel S, Beljanski V, Van Grevenynghe J et al (2013) BCL-2 Inhibitors Sensitize Therapy-resistant Chronic Lymphocytic Leukemia Cells to VSV Oncolysis [J]. Mol Ther 21(7):1413–1423
26. Wei Y, Pattingre S, Sinha S et al (2008) JNK1-Mediated Phosphorylation of Bcl-2 Regulates Starvation-Induced Autophagy [J]. Mol Cell 30(6):678–688
27. Cao DS, Jiang SL, Guan YD et al (2020) A multi-scale systems pharmacology approach uncovers the anti-cancer molecular mechanism of Ixabepilone [J]. Eur J Med Chem 199:112421
28. Buzea C, Blandino IIP, Robbie K (2007) Nanomaterials and nanoparticles sources and toxicity [J]. Biointerphases 2(4):MR17–MR172

29. Yang D, Zhang M, Gan Y et al (2020) Involvement of oxidative stress in ZnO NPs-induced apoptosis and autophagy of mouse GC-1 spg cells [J]. Ecotoxicol Environ Saf 202:110960
30. Zhao X, Ren X, Zhu R et al (2016) Zinc oxide nanoparticles induce oxidative DNA damage and ROS-triggered mitochondria-mediated apoptosis in zebrafish embryos [J]. Aquat Toxicol 180:56–70
31. Akhtar MJ, Ahamed M, Kumar S et al (2012) Zinc oxide nanoparticles selectively induce apoptosis in human cancer cells through reactive oxygen species. [J]. Int J Nanomed 7:845–57
32. Xia T, Kovochich M, Brant J, et al (2006) Comparison of the abilities of ambient and manufactured nanoparticles to induce cellular toxicity according to an oxidative stress paradigm. J Nano Lett 6(8):1794–807
33. Kong T, Zhang SH, Zhang JL et al (2018) Acute and Cumulative Effects of Unmodified 50-nm Nano-ZnO on Mice [J]. Biol Trace Elem Res 185(1):124–134
34. Chen P, Wang H, He M et al (2019) Size-dependent cytotoxicity study of ZnO nanoparticles in HepG2 cells [J]. Ecotoxicol Environ Saf 171:337–346
35. Kim KM, Kim MK, Paek HJ et al (2016) Stable fluorescence conjugation of ZnO nanoparticles and their size dependent cellular uptake [J]. Colloids Surf B Biointerfaces 145:870–877
36. Deylam M, Alizadeh E, Sarikhani M et al (2021) Zinc oxide nanoparticles promote the aging process in a size-dependent manner [J]. J Mater Sci Mater Med 32(10):128
37. Egbuna C, Parmar VK, Jeevanandam J et al (2021) Toxicity of Nanoparticles in Biomedical Application: Nanotoxicology [J]. J Toxicol 2021:9954443